Acta Crystallographica Section B
Structural Science
ISSN 0108-7681

Coherence length of the $KY(WO_4)_2$ single crystal

A. Shalimov,[a] M. T. Borowiec,[a]* T. Zayarnyuk,[a] M. C. Pujol,[b] M. Aguiló[b] and F. Díaz[b]

[a]Institute of Physics, Polish Academy of Sciences, Al. Lotników 32/46, Pl 02-668, Warsaw, Poland, and [b]Física i Cristal·lografia de Materials (FiCMA), Universitat Rovira i Virgili (URV), Campus Sescelades c/Marcel·lí Domingo, s/n, E-43007-Tarragona, Spain

Correspondence e-mail: borow@ifpan.edu.pl

Received 20 December 2007
Accepted 3 April 2008

Potassium yttrium tungstate is a monoclinic crystal with space group *C*2/*c*. The specific X-ray investigations presented in this article determine the coherence scattering length for this crystal. The scattering profiles were obtained using a Philips MRD X-ray diffractometer. The Williamson–Hall method was used to determine the coherence scattering length and internal stresses.

1. Introduction

Diode-laser-pumped solid-state laser devices have a variety of applications owing to the versatility of the process. A number of crystalline hosts (more than 280) have been developed with rare-earth ions, transition metals and actinides (Kaminiski & Kaminskii, 1996; Kaminskii, 2003). There is little real application in the laser world for parameters such as overall efficiency, average power, thermal lensing, optical and mechanical stability. Potassium yttrium tungstate [$KY(WO_4)_2$, hereinafter KYW] single crystals offer an unusual wealth of properties, such as a large cross section, when they are doped with lanthanides and some of these physical properties exhibit an interesting anisotropy. KYW biaxial crystals are also called self-active lasers, since the rare-earth ion laser emission and the stimulated Raman scattering (SRS) occur inside the same crystal (Griebner *et al.*, 2005; Grabtchikov *et al.*, 2002; Han *et al.*, 2002; Metrat *et al.*, 1997; Gallucci *et al.*, 1998). The physical characteristics of the majority of crystals depend on their structural properties and defect structures. The development of crystal growth technology will require further structural investigation.

The measurements of coherence length in a relatively large single crystal of KYW is of great importance because it can be used as a reference point for a subsequent study involving the determination of the sizes of nanocrystals (Borowiec *et al.*, 2006). The grain size of nanocrystals of a given material cannot be measured accurately using the X-ray method unless the coherence length of the bulk material is known.

For nearly perfect crystals, such as Si or GaAs, the length of coherence scattering mainly depends on the spectral purity of the radiation (Holy *et al.*, 1999). Considering that, the ratio of the wavelength dispersion to the radiation wavelength, $\Delta\lambda\backslash\lambda$, is *ca* 10^{-5}–10^{-6} for a triple crystal diffractometer, and the coherence scattering length for nearly perfect crystals reaches tens of microns and defines the upper limit for the determination of coherence block size.

2. Samples and experiment

This paper is concerned with the most relevant structural phase of the potassium rare-earth tungstate (KREW)

$KLn(WO_4)_2$, where Ln–Y, Gd–Lu, for laser applications. This monoclinic phase with space group $C2/c$ belongs to the centrosymmetric $2/m$ Laue class (Pujol *et al.*, 2001). Unit-cell parameters are $a = 10.64$, $b = 10.35$, $c = 7.54$ Å and $\beta = 130.5^\circ$ with $Z = 4$ (Borisov & Klevtsova, 1968). The monoclinic structure of the KREW is characterized by a double chain of W_2O_8 (two octahedral WO_4^{2-} anionic complexes sharing edges) along the **c** direction. The K^+ and Y^{3+} cations occupy C_2 positions and are surrounded by 12 and eight O atoms, respectively. The coordination and local symmetry of the Y^{3+} cation is particularly interesting owing to the fact than the active lanthanide ion substitutes this ion. The structure of potassium yttrium tungstate is described in more detail by Pujol *et al.* (2001), Borisov & Klevtsova (1968) and Klevtsov *et al.*, 1968).

Monoclinic KYW crystals were grown using the top-seeded solution growth-slow cooling (TSSG-SC) method as described in previous work on other members of the monoclinic double tungstate KREW family of compounds (Solé *et al.*, 1996; Aznar *et al.*, 2004; Mateos *et al.*, 2006). The crystal growth was carried out using $K_2W_2O_7$ as a solvent. Supersaturation was obtained by slowly cooling the solution from the saturation temperature. The solution composition was 12 mol % KYW/88 mol % $K_2W_2O_7$. This was chosen in view of the solubility curve of KYW in $K_2W_2O_7$ (Tu *et al.*, 1994).

The crystals were grown from *ca* 200 g of solution prepared in 125 cm^3 cylindrical platinum crucibles. The reagents were 99.9% pure K_2CO_3, Y_2O_3 and WO_3. The solution was homogenized by maintaining the temperature at around 50 K above the expected temperature of saturation for several hours.

The axial temperature gradient in the solution was 1.5 K cm^{-1}, with the surface cooler than the bottom. The thermal gradients in the solutions were approximately 1.5 and 1 K cm^{-1} for the axial and radial gradients, respectively. The bottom and the crucible wall were the hottest parts. The growth of double tungstates is very sensitive to thermal gradients (Majchrowski *et al.*, 2003). Large thermal gradients may cause the growing crystal to crack owing to the high anisotropy of the linear thermal expansion coefficients of monoclinic double tungstates. After homogenization of the solution, the saturation temperature was determined by observing the growth/dissolving of the seed, to be around 1190 K.

We grew a single crystal in the centre of the surface of the solution with the [010] crystallographic direction perpendicular to the surface of the solution. The temperature of the solution was decreased at a rate of 0.1–0.2 K h^{-1} for 20–28 K from the saturation temperature. The crystal rotation was 40 r.p.m. without pulling. After 6 or 8 d of growth, the crystal was removed from the solution and maintained just above the surface of the solution, while the entire growth system was cooled to room temperature at a rate of 25–30 K h^{-1} to avoid thermal stresses.

The X-ray measurements were carried out with a Philips MRD high-resolution X-ray diffractometer (Fig. 1 is a schematic representation) using Cu $K\alpha_1$ radiation ($\lambda = 1.5406$ Å). The diffractometer was equipped with a Bartels mono-

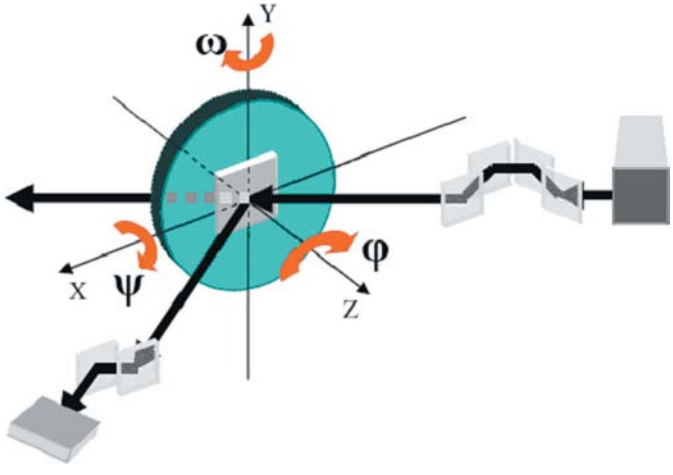

Figure 1
High-resolution Philips MRD X-ray diffractometer.

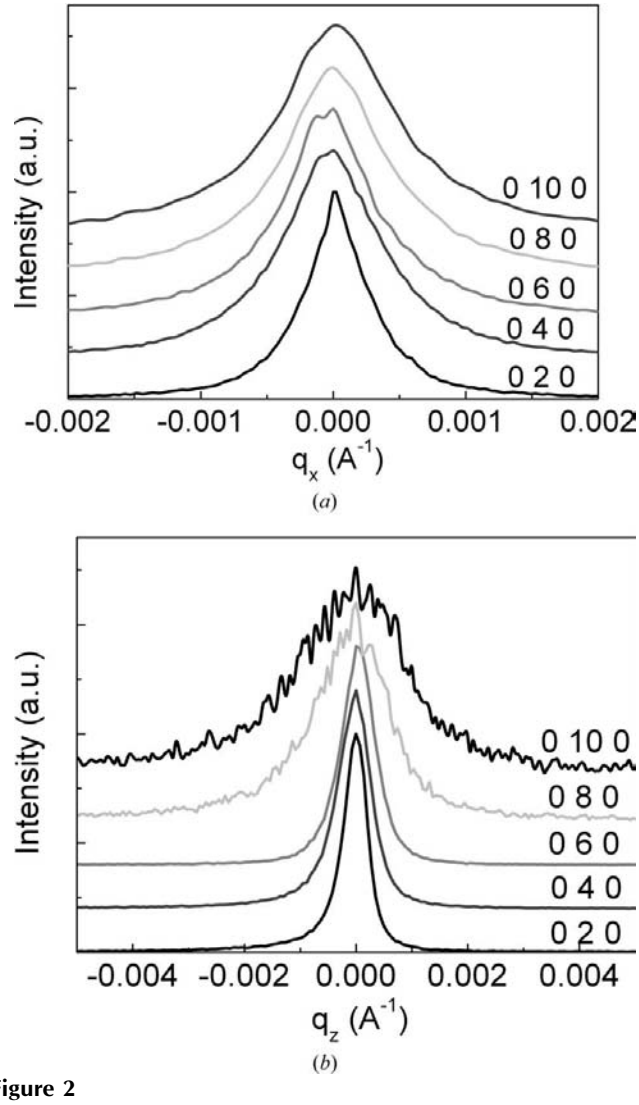

Figure 2
Intensity distributions along (*a*) q_x and (*b*) q_z directions for the set of (0*k*0) reflections.

chromator and a two-crystal Ge220 analyser. The (020), (040), (060), (080), (0,10,0) were examined after carrying out the standard sample adjustment procedure. The measurements were performed in the double (rocking curves) and triple axis geometries of the diffractometer to record reciprocal space maps (RLMs), and to perform longitudinal ($2\theta/\omega$) and transverse (ω) scans.

To determine the coherence scattering length, Λ, of the $KY(WO_4)_2$ crystal, a set of intensity distribution measurements was taken along the **x** and **z** directions, perpendicular and parallel to a reciprocal lattice vector, **Q**, respectively. The components of the **Q** and q (deviation from the reciprocal lattice vector) vectors can be expressed in terms of the angle between the incoming beam and the sample surface α_i, the angle between the diffracted beam and the surface α_f, and the respective deviations $\Delta\alpha_i$ and $\Delta\alpha_f$ from the diffraction maximum

$$\begin{aligned} Q_x &= \frac{2\pi}{\lambda}\left(\cos\alpha_f - \cos\alpha_i\right);\\ q_x &= \frac{2\pi}{\lambda}\left(\Delta\alpha_i \sin\alpha_i - \Delta\alpha_f \sin\alpha_f\right);\\ Q_z &= \frac{2\pi}{\lambda}\left(\sin\alpha_i + \sin\alpha_f\right);\\ q_z &= \frac{2\pi}{\lambda}\left(\Delta\alpha_f \cos\alpha_f + \Delta\alpha_i \cos\alpha_i\right). \end{aligned} \tag{1}$$

The transverse and longitudinal scans of the set of reflections were obtained with the diffractometer in the triple axis mode. These are presented in Fig. 2.

The coherent length values, Λ_x and Λ_z, perpendicular and parallel to the growth direction [010], were calculated using the dependence of Λ on the diffraction peak width Δq described by the formulae (Krivoglaz, 1967)

$$\langle\Delta q\rangle = \frac{2\pi}{\langle\Lambda\rangle};\ \Delta q_x = \frac{2\pi}{\Lambda_x};\ \Delta q_y = \frac{2\pi}{\Lambda_y};\ \Delta q_z = \frac{2\pi}{\Lambda_z}. \tag{2}$$

Plotting Δq values for different reflections against the modulus of the reciprocal lattice vector **Q** for the corresponding reflections revealed an almost linear dependence (Fig. 3). Therefore, interpolation of the fitted lines along the Δq axis gives the inverse coherence lengths, while the gradient of the straight line is proportional to the internal strain of the crystal.

The Williamson–Hall method was used to determine the coherence scattering length and internal stresses (Williamson & Hall, 1953). The lateral coherence scattering length, Λ_x, was found to be 2.1 µm, compared with a coherence scattering length, Λ_z, along the growth direction of 3.4 µm. Coherence

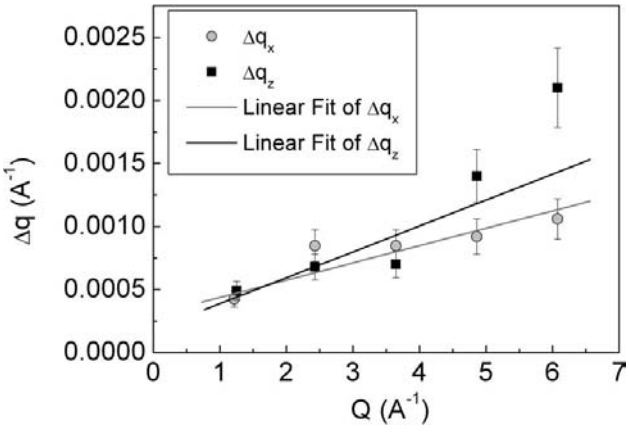

Figure 3
Dependence of peak widths Δq on the absolute value of **Q** (Williamson–Hall plot).

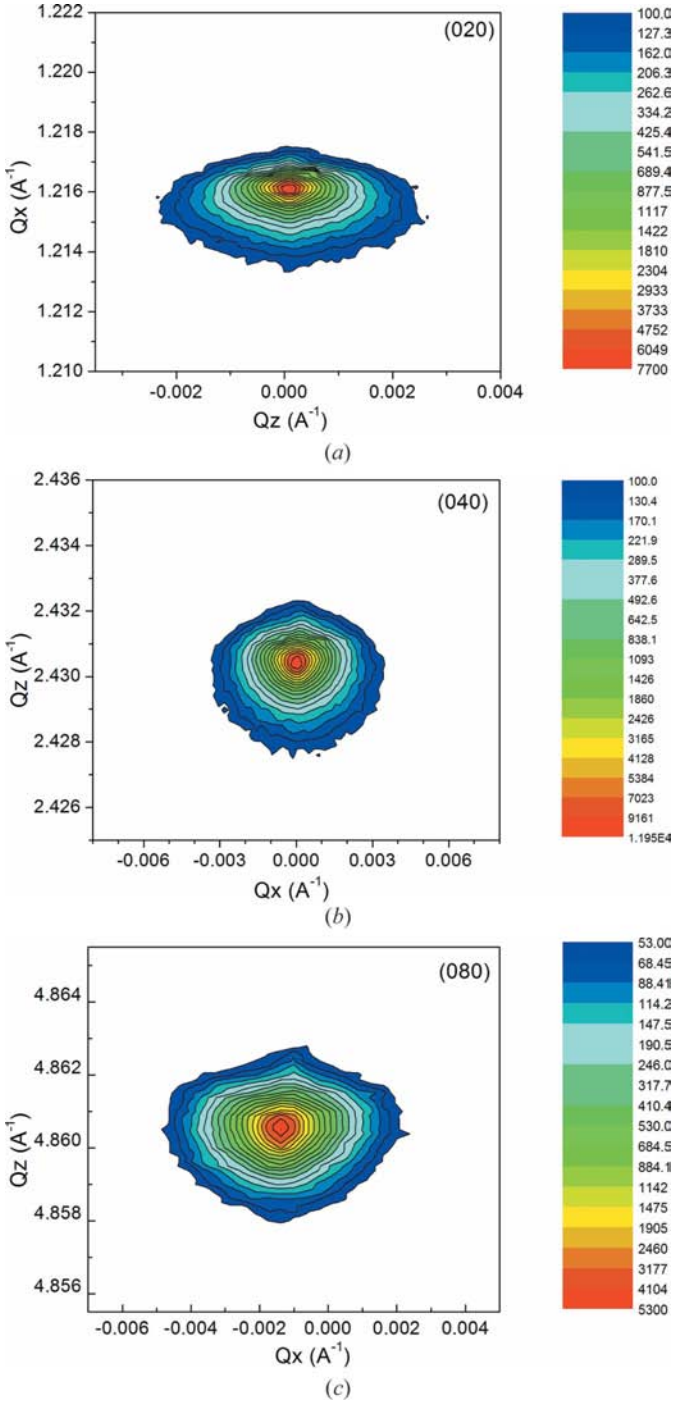

Figure 4
Reciprocal space maps for (020), (040) and (080) reflections.

scattering lengths can be slightly overestimated owing to the simplicity of the diffraction peak-broadening model. A detailed analysis of grain sizes and the effects of internal stresses on peak widths using more advanced X-ray diffraction techniques (Balzar, 1992; Ungar & Borbely, 1996) is needed. Such an analysis would have to allow for the strain non-uniformity of crystal lattices (Shalimov *et al.*, 2007). We also should note that the instrumental width of the diffractometer equipped with a Bartels monochromator gives a beam divergence of 12". Assuming that the diffracted peaks are represented by a combination of Gaussian contributions for the instrumental function and 'pure' scattering from the crystal, we estimated the peak width caused only by the X-ray scattering from the crystal. Knowing that the measured FWHM of the (0,10,0) ω scan is 35.2", then the 'pure' FWHM of this reflection is equal to $(35.2^2 - 12^2)^{1/2} = 33.09$ (arc s), which differs insignificantly from the measured FWHM value. For other reflections this difference will be less, because the (0,10,0) is the narrowest (in angular units, the broadest in q space) diffraction peak.

The diffracted intensity distributions are characterized by relatively large Δq values and do not contain the Dirac δ function term. This effect is typical for dislocation-contained crystals (Krivoglaz, 1967). It is well known that asymmetry in X-ray diffuse scattering from 'weak' defects is described by the complex term in the equation for the amplitude of a scattered wave (Krivoglaz, 1996; Pietsch *et al.*, 2004; Larson, 1975; Dederichs, 1971). Moreover, the fact that the reciprocal space map (RSM; Fig. 4) is asymmetric along $\mathbf{Q}z$ points to defects that cause a negative volume dilation (vacancies, dislocation loops of vacancy type *etc.*; Krivoglaz, 1967). The reason that vacancy-type defects (probably small dislocation loops) are so prevalent in these crystals could be specific to the structure of $KY(WO_4)_2$, which consists of complexes of metallic cations surrounded by several oxygen anions. If during TSSG-SC growth, some metallic atoms do not occupy their positions, only oxygen complexes appear. Such complexes could lead to the generation of small dislocation loops of vacancy type.

3. Conclusions

The coherence scattering lengths in the directions parallel and perpendicular to the growth directions were estimated from the broadening of X-ray reflections. Relatively large dimensions (2.1×3.4 µm) of coherence crystalline blocks were found. Qualitative analysis of the shape of the diffracted peaks and of the intensity distribution in reciprocal space maps indicated the presence of dislocations and volume defects, which introduced a negative dilation into the crystal host.

The reciprocal lattice vector **Q** for the corresponding reflections has a near linear dependence of peak widths Δq on the absolute value of **Q**. The lateral length of coherence scattering along the growth direction was established.

This work was supported by EU project DT-CRYS, NMP3-CT-2003-505580, by Polish State Committee on Science (KBN; decision of project No. 72/E-67/SPB/6. PR/DIE 430/2004-2006).

References

Aznar, A., Solé, R., Aguiló, M., Díaz, F., Griebner, U., Grunwald, R. & Petrov, V. (2004). *Appl. Phys. Lett.* **85**, 4313–4315.
Balzar, D. (1992). *J. Appl. Cryst.* **25**, 559–570.
Borisov, S. V. & Klevtsova, R. F. (1968). *Sov. Phys. Crystallogr.* **13**, 420–421.
Borowiec, M. T., Deptuła, A., Lojkowski, W., Gierlotka, S., Dyakonov, V. P., Lada, W., Olczak, T., Wawszczak, D., Aleshkevych, P., Domuchowski, W., Zayarnyuk, T., Barański, M., Czech, M. & Szymczak, H. (2006). *Solid State Phen.* **128**, 25–30.
Dederichs, P. H. (1971). *Phys. Rev. B*, **4**, 1041–1050.
Gallucci, E., Goutaudier, C. & Boulon, G. (1998). *Eur. J. Solid State Inorg. Chem.* **35**, 433–446.
Grabtchikov, A. S., Kuzmin, A. N., Lisinetskii, V. A., Orlovich, V. A., Demidovich, A. A., Danailov, M. B., Eichler, H. J., Bednarkiewicz, A., Strek, W. & Titov, A. N. (2002). *Appl. Phys. B*, **75**, 795–797.
Griebner, U., Liu, J., Rivier, S., Aznar, A., Grunwald, R., Sole, R., Aguilo, M., Diaz, F. & Petrov, V. (2005). *IEEE J. Quantum Electron.* **41**, 408–414.
Han, X., Wang, G. & Tsuboi, T. (2002). *J. Cryst. Growth*, **242**, 412–415.
Holy, V., Pietsch, U. & Baumbach, T. (1999). *High-Resolution X-ray Scattering from Thin Films and Multilayers*, p. 28. Berlin: Springer.
Kaminiski, A. A. & Kaminskii, A. (1996). *Crystalline Laser, Physical Processes and Operating Schemes*, pp. 499–501. London: CRC Press.
Kaminskii, A. A. (2003). *Phys. Status Solidi A*, **200**, 215–296.
Klevtsov, P. V., Kozeeva, L. P. & Klevtsova, R. F. (1968). *Inorg. Mater.* **4**, 1147–1149.
Krivoglaz, M. A. (1967). *Theory of X-ray and Thermal Neutron Scattering.* Moscow: Nauka.
Krivoglaz, M. A. (1996). *X-ray and Neutron Diffraction in Nonideal Crystals.* Berlin: Springer.
Larson, B. C. (1975). *J. Appl. Cryst.* **8**, 150–160.
Majchrowski, A., Borowiec, M. T. & Michalski, E. (2003). *J. Cryst. Growth*, **264**, 201–207.
Mateos, X., Solé, R., Gavaldà, J., Aguiló, M., Massons, J. & Díaz, F. (2006). *Opt. Mater.* **28**, 423–431.
Metrat, G., Muhlstein, N., Brenier, A. & Boulon, G. (1997). *Opt. Mater.* **8**, 75–82.
Pietsch, U., Holy, V. & Baumbach, T. (2004). *High-Resolution X-ray Scattering/From Thin Films to Lateral Nanostructures.* Berlin: Springer.
Pujol, M. C., Solé, R., Massons, J., Gavaldà, Jna., Solans, X., Zaldo, C., Díaz, F. & Aguiló, M. (2001). *J. Appl. Cryst.* **34**, 1–6.
Shalimov, A., Bak-Misiuk, J., Kaganer, V. M., Calamiotou, M. & Georgakilas, A. (2007). *J. Appl. Phys.* **101**, 013517.
Solé, R., Nikolov, V., Ruiz, X., Gavaldà, J., Solans, X., Aguiló, M. & Díaz, F. (1996). *J. Cryst. Growth*, **169**, 600–603.
Tu, C., Huang, Y., Luo, Z. & Chen, G. J. (1994). *Cryst. Growth*, **135**, 636–641.
Ungar, T. & Borbely, A. (1996). *Appl. Phys. Lett.* **69**, 3173–3175.
Williamson, G. K. & Hall, W. H. (1953). *Acta Metall.* **1**, 22–30.